MATERIALE PLASTICE
https://revmaterialeplastice.ro
https://doi.org/10.37358/Mat.Plast.1964

CC BY

Multiscale Strengthening of Fast-Growing Wood for Lightweight, High-Strength Structural Applications: From Cell-Wall Engineering to Reconstitution

MINTING LAI[1,2,3], LAMEI LI[1,2,3], YIXIN LI[1,2,3], WANJU LI[1,2,3], QIAOGUANG LI[4], GUIJUN XIE[1,2,3]*

[1] Institute of Comprehensive Utilization of Forest Resources, Guangdong Academy of Forestry, Guangzhou, China
[2] Guangdong Provincial Key Laboratory of Forest Silviculture, Protection and Utilization, Guangzhou, China
[3] Key Laboratory of National Forestry and Grassland Administration on Ecosystem Conservation and Restoration in the Guangdong-Hong Kong-Macao Greater Bay Area, Guangzhou, China
[4] College of Chemical and Materials Engineering, Zhongkai University of Agriculture and Engineering, Guangzhou, China

Abstract: *Fast-growing plantation woods, including poplar, Chinese fir, pine, and eucalyptus, are abundant and rapidly renewable resources. However, their low density, high porosity, and comparatively weak interpolymer interactions limit their direct use in demanding structural applications. This review examines recent strategies for upgrading fast-growing wood through cell-wall engineering and structural reconstitution, including partial delignification followed by thermo-hydro-mechanical densification, pressure-free self-densification, bottom-up reconstitution, scrimber-based assembly, and spatially programmed densification. The strengthening mechanisms are organized across four coupled length scales: molecular-scale hydrogen-bonding reconfiguration and cellulose crystallinity; cell-wall collapse and pore elimination; fibre-bundle alignment and microfibril-angle regulation; and interfacial bonding and bulk stress transfer. Rather than acting independently, these mechanisms jointly determine the balance among density, strength, toughness, dimensional stability, and functional performance. The review further discusses current challenges in comparing reported properties across studies, moisture-induced performance loss, scalable manufacturing, and life-cycle sustainability. Reported gains are large but scale-dependent: partial delignification with hot-pressing raises strength more than tenfold, self-densified and reconstituted woods reach tensile strengths of roughly 500–590 MPa, and thin delignified films exceed 340 MPa, yet these absolute gains come with densities roughly three times that of native wood and remain vulnerable to moisture-driven set-recovery. We conclude that establishing standardized testing and reporting practices, together with predictive multiscale models, will be essential for translating engineered fast-growing wood into reliable lightweight structural materials.*

Keywords: *Fast-growing wood, wood densification, delignification, cell-wall engineering, reconstituted wood, multiscale structure-property relationships, structural biomaterials*

1. Introduction

The decarbonization of the built environment has turned wood from a traditional commodity into a strategic structural material. Cement and steel together account for a large share of industrial carbon dioxide (CO_2) emissions. Substituting them with wood-based load-bearing components can reduce whole-building emissions by roughly two-thirds relative to conventional construction, while storing biogenic carbon in service [1]. Scenario analyses of timber cities and the global scale-up of mass-timber products project net emission reductions of tens of gigatonnes of CO_2-equivalent ($GtCO_2e$) over the century, together with expanded forest carbon stocks [2,3]. These prospects have driven intense effort to engineer wood beyond its native performance, so that renewable lignocellulose can compete with metals in stiffness- and strength-critical applications [4].

**email: xgj80@126.com*

Realizing this vision at scale hinges on the feedstock. Slow-grown, high-density hardwoods are limited in supply. Fast-growing plantation species, such as poplar, Chinese fir, pine and eucalyptus, together with fast-growing invasive species of rising interest such as tree-of-heaven (*Ailanthus altissima*) [5], are abundant, cheap and carbon-efficient, yet mechanically weak. Their low density (commonly around 0.3–0.5 g cm^{-3} for the principal plantation species; see Table 1), high porosity and, in juvenile wood, large microfibril angle (MFA) translate into low modulus and strength and a marked tendency to buckle and collapse under load [6]. These limitations are set hierarchically. The multilayered secondary cell wall, its cellulose crystallinity and MFA, and the porous tissue architecture jointly govern macroscopic behaviour across roughly five orders of magnitude in modulus [7–11]. Because this hierarchy is the origin of the weakness, it is also the design space in which strengthening can be engineered.

Two broad strategies have emerged. The first, cell-wall engineering, partially removes lignin and hemicellulose and then densifies the softened wall by thermo-hydro-mechanical (THM) hot-pressing. The landmark demonstration raised strength more than tenfold while retaining residual lignin as a bonding phase [12], and a later water-shock route enabled cold, moldable three-dimensional shaping of lightweight wood [13]. The second strategy moves beyond hot-pressing. Self-densification by controlled swelling and air-drying yields isotropic bulk wood with tensile strengths approaching 500 MPa without external pressure [14,15]. Reconstitution and assembly routes, such as scrimber from defibrated bundles and asymmetric or gradient densification, reorganize the fibre network into structural composites whose properties are dominated by the attained density [16–18]. One tension cuts across both strategies: densification raises strength but sacrifices the lightweight, porous character that makes wood attractive, and different routes negotiate this lightweight–strength trade-off in different, often incompatible, ways.

Existing reviews have surveyed these advances, but mostly organize them by processing route or by end property, such as transparent wood, densified wood, cellulose scaffolds and functional derivatives [4,19–21]. Two things are missing. One is a mechanistic through-line that explains why these disparate treatments work in common terms. The other is a focus on the low-value fast-growing feedstock, where the industrial and climate payoff is largest [22]. As a result, strengthening outcomes are often reported as route-specific empirical gains rather than as expressions of shared, scale-spanning physics.

This review is organized around that missing axis. We treat the strengthening of fast-growing wood as a single problem of structural control transmitted across four coupled length scales: molecular hydrogen bonding and crystallinity, cell-wall collapse and densification, fibre orientation and stacking, and inter-fibre interfacial bonding [23–26]. Within this framework we integrate delignification, THM densification, self-densification, reconstitution and gradient design as alternative means of tuning the same underlying levers (Figure 1). The central argument is that these levers are coupled, not additive: a single densification step moves several at once, which is why chemically distinct routes converge on comparable strength. We then use it to rationalize the lightweight–strength trade-off, dimensional stability and multifunctionality. By centring the analysis on abundant plantation species, the review aims to connect mechanistic understanding with the scalable upgrading of low-value wood into lightweight, high-strength structural materials.

2. Literature search and scope

This article is a narrative, mechanism-oriented review rather than a systematic review. Relevant literature was identified through targeted searches of major publisher databases (Elsevier ScienceDirect, Springer Nature, the American Chemical Society, Wiley, MDPI, the Multidisciplinary Digital Publishing Institute, and AAAS/Science, the American Association for the Advancement of Science) together with the Crossref metadata registry, using combinations of keywords including fast-growing wood, plantation wood, wood densification, delignification, cell-wall engineering, reconstituted wood, scrimber, thermo-hydro-mechanical treatment and multiscale strengthening mechanism. The search covered publications up to 2026 and was extended by backward and forward citation tracking of key papers. Sources were

CC BY

included when they were peer-reviewed studies directly addressing the strengthening, densification, reconstitution or multiscale mechanics of fast-growing wood and closely related lignocellulose. Priority was given to landmark studies that established the principal strengthening routes and to recent primary research from 2020 to 2026 reporting quantitative structure–property data. Review articles were retained only to frame context. Non-peer-reviewed material and studies lacking extractable mechanistic or quantitative content were excluded. For every retained source, the bibliographic metadata (title, authors, year and digital object identifier (DOI)) were verified against Crossref, and the specific statement attributed to it was checked against the corresponding abstract or full text. In practice the selection proceeded in three steps: candidate records were first identified from these databases, then screened by title and abstract for direct relevance to the strengthening of fast-growing wood, and finally assessed in full text for extractable mechanistic or quantitative content. The resulting evidence base comprises 91 sources spanning 2000 to 2026, of which about 68% were published between 2020 and 2026.

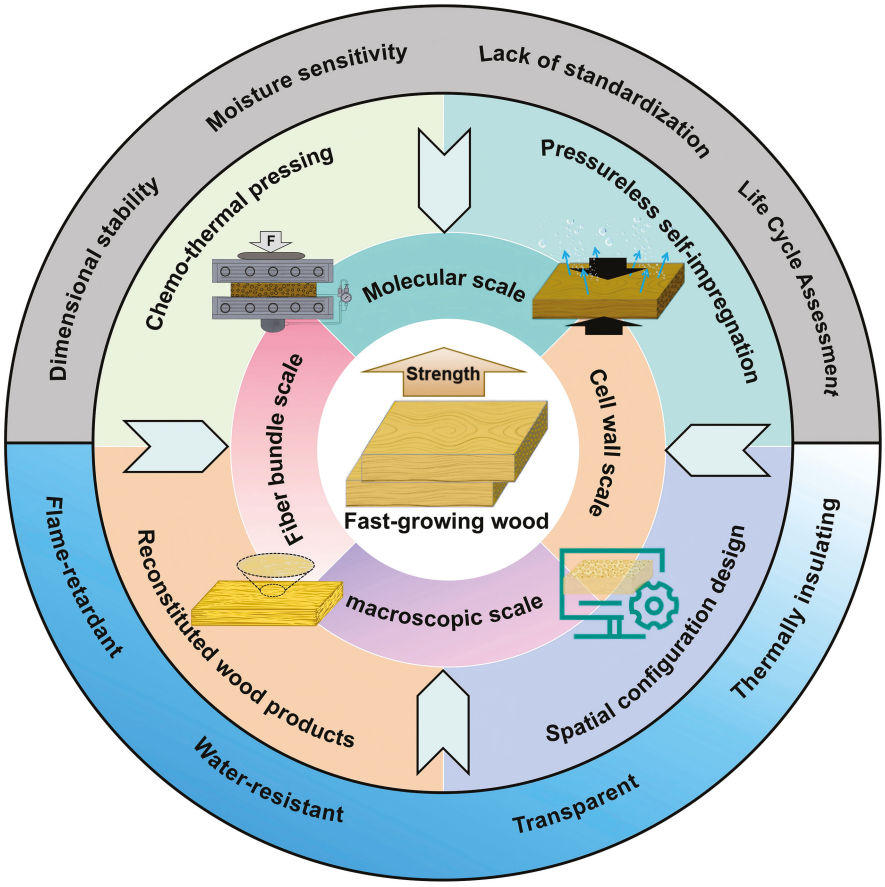


Figure 1. Wood processing technologies and material properties

3. Wood processing technology

3.1. Cell-wall engineering: delignification and densification

Cell-wall engineering upgrades wood through two coupled operations: selective removal of matrix polymers, and thermo-hydro-mechanical (THM) densification. Together they reconstruct the secondary wall at its own length scale. In the landmark demonstration, partial delignification followed by hot-pressing raised the strength of natural wood more than tenfold. That result established both the potential of the approach and its governing design variable, namely how much lignin and hemicellulose are

removed before the softened wall is consolidated [4,12]. Whether the route yields a strong structural solid or a weak, over-processed one is decided largely at this first step. So it is the chemistry and extent of delignification, not the pressing conditions on their own, that we take as the organizing axis for the strategy.

The response to these two operations is not uniform across the feedstock, because wood anatomy and lignin chemistry differ systematically among the botanical groups from which fast-growing species are drawn. Gymnosperm softwoods such as pine and Chinese fir are built almost entirely from axial tracheids and carry guaiacyl-rich lignin at about 26–32%, which resists delignification comparatively strongly. Dicotyledonous hardwoods such as poplar and eucalyptus combine thick-walled fibres with large-diameter vessels and carry syringyl-guaiacyl lignin at about 20–25%, which is removed more readily. In a controlled comparison at matched initial density, delignification was roughly twice as efficient in aspen as in Scots pine, yet the two reached almost identical compression ratios while the hardness and compressive-strength gains were larger in the hardwood [27]. Monocotyledons such as bamboo, though not true wood, are frequently processed alongside these species; their scattered vascular bundles and lack of secondary growth present a different starting architecture that a sodium-hydroxide-only route can nonetheless plasticize across several species [28]. The strengthening levers discussed in Section 4 therefore act on every group, but the ease of delignification and the achievable degree of densification are set by these anatomical and compositional starting points.

What polymer is removed, by what chemistry, and to what extent: these fix the starting state for wall reconstruction. Partial delignification, by alkaline sulfite, deep eutectic solvents (DES) or hydroxide treatments, dissolves lignin together with part of the hemicellulose while leaving the cellulose skeleton intact. This opens the wall to plastic collapse and increases chain mobility. The effect of removal degree is non-monotonic. Eliminating 50–80% of the lignin raises crystallinity by 21–54% as freed microfibrils reorganize into closer registry, whereas more aggressive treatment begins to damage the crystalline region itself and erodes the load path it was meant to expose [29]. Green DES routes reach comparable partial removal with milder, recyclable chemistry (Figure 2) [30,31]. Ionic-liquid treatments that partially dissolve the fibre surface add a distinct route to re-bondable all-wood composites [32,33]. Push removal to the other extreme and near-complete delignification leaves a nanoporous, purely cellulosic template [34], valuable for functional materials but, as shown below, mechanically a different kind of material from the partially delignified state. The reason the two families of matrix polymer matter is that they play complementary roles. Hemicellulose, the more hydrophilic and thermally labile of the two, largely controls how the wall softens: removing part of it lowers the effective glass-transition temperature and enhances plasticization, so the wall yields and collapses more readily under moderate heat and pressure [35]. Lignin removal governs something else: how far the freed microfibrils can reorganize, and how much bonding capacity survives. Best, then, to remove the two to different, independently tuned extents rather than stripping them in fixed proportion [29].

Each chemistry attacks something different, and so leaves the wall in a different state. Alkaline-sulfite and related pulping-derived treatments cleave the aryl-ether linkages of lignin and sulfonate the residual fragments. They produce a swollen but structurally continuous wall that collapses readily under pressing [12]. Deep eutectic solvents, formed from hydrogen-bond donor–acceptor pairs, disrupt the lignin–carbohydrate associations under milder, recyclable conditions while largely sparing the cellulose skeleton [31]. Ionic liquids act more aggressively, partially dissolving and re-precipitating cellulose at the fibre surface to create a bondable skin that welds neighbouring cells on consolidation [32,33]. Since each route removes lignin and hemicellulose in different proportions, one nominal delignification degree can hide quite different residual architectures. That is a large part of why strengths reported at matched removal levels still scatter between studies, and why removal degree alone describes the treated state only incompletely [29].

Densification then turns the porosity of the softened wall into intrinsic wall strength. Under combined heat and moisture the matrix polymers soften toward their glass transition. Hot-pressing collapses

the lumen and stacks the wall layers into a near-void-free solid; the classical THM treatment raised longitudinal shear strength more than tenfold by this mechanism alone [35,36]. Because the modulus and strength of a cellular solid scale steeply with relative density, the removal of porosity is itself a first-order source of the gain, on which the reorganization of the wall polymers builds [12,20]. The two operations are sequential but tightly coupled. Prior delignification governs how far the wall can be collapsed and how closely the microfibrils are brought together during pressing, so pressing conditions and removal degree cannot be optimized independently (Figure 3).

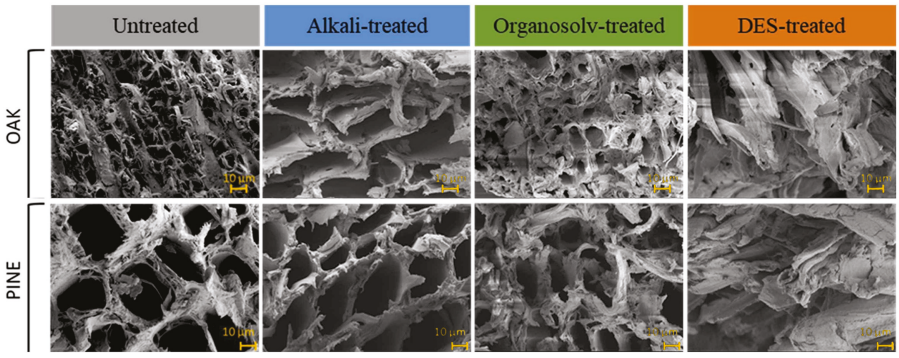


Figure 2. Scanning electron micrographs of oak (top row) and pine (bottom row) wood, untreated and after alkali, organosolv and deep eutectic solvent (DES) pretreatment, comparing the cell-wall morphology produced by each pretreatment; Scale bars, 10 μm. Images were acquired by field-emission scanning electron microscopy (SEM) at 3 kV (Zeiss Ultra Plus). Adapted from Ref. [30]

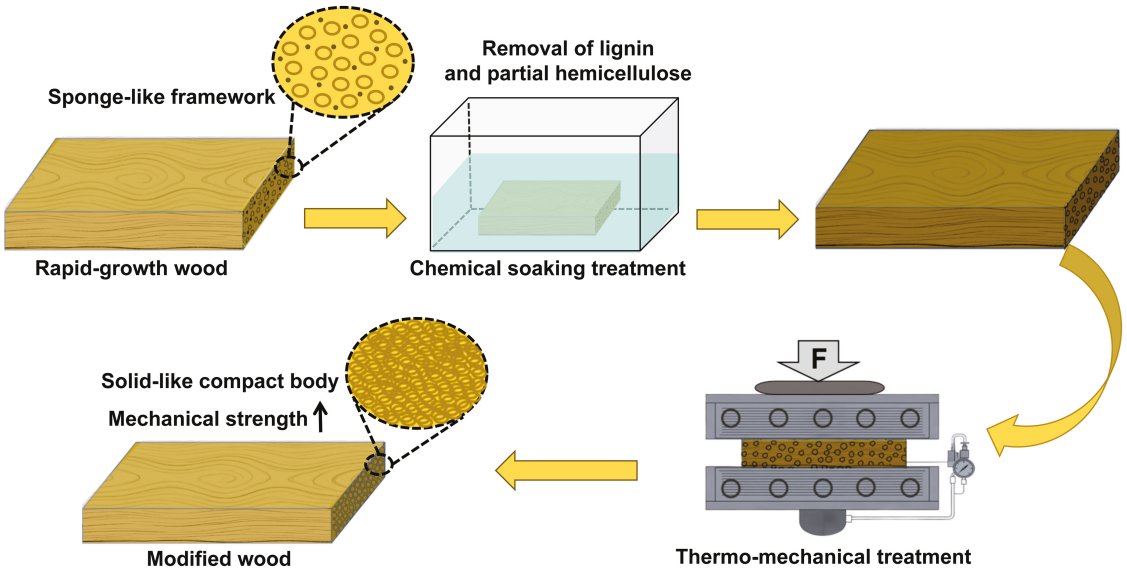


Figure 3. Thermo-mechanical treatment of wood

The pressing step has a narrow operating window, set by the thermal softening of the wall polymers. Lignin and hemicellulose both plasticize as temperature rises in the moist state, and their glass transitions fall steeply with moisture content. Pressing is therefore done above this softened threshold, with the platens held until the collapsed geometry sets [35]. Push the temperature or moisture too low and the wall stays too stiff to collapse, fracturing instead. Push the heat too high and the polymers degrade and

the material darkens. Delignification narrows the window further: a wall stripped of its matrix collapses under milder conditions, yet the same stripping removes the binder that fixes the pressed shape. Removal chemistry and thermomechanical pressing are coupled here, so densification is a joint optimization rather than two separable steps [20,36].

Where removal is balanced against retention sets the central design boundary of the strategy. Retaining a fraction of lignin preserves an in-wall bonding phase that welds adjacent microfibrils and fibres as pressing brings them together, and this residual binder is what lets the partially delignified, hot-pressed material reach full strength instead of delaminating [12]. Complete removal follows a different logic. Once densified, the resulting pure-cellulose bulk can show excellent intrinsic tensile properties [37]; with its native binder gone, however, it usually needs an infiltrated polymer to transfer load, as in delignified wood–epoxy interpenetrating composites, whose stiffness and strength exceed the rule of mixtures [38]. Lignin-retaining templates stay stronger as scaffolds than their fully delignified counterparts, which confirms that lignin contributes structurally and not merely optically [39]. The practical optimum therefore sits at an intermediate degree rather than at maximal delignification: enough matrix is removed to permit collapse, and enough lignin is kept to bond the consolidated wall. Its exact position shifts with species, chemistry and target property.

At the processing level, what this optimum controls is the quantity and continuity of the in-wall binder: retained lignin re-bonds the consolidated wall without any added adhesive [12], whereas a fully delignified template must instead be re-infiltrated with a synthetic polymer to supply the same load-transferring phase [37,38]. The molecular basis of this bonding, and its quantitative optimum, is examined at the interfacial and bulk scale in Section 4.4.

Vary the removal chemistry and the pressing conditions around this optimum, and one two-step logic gives rise to a broad family of structural materials. Partial delignification and hot-pressing of thin sections yield sub-ten-micrometre wood films with a tensile strength of 342 MPa and a modulus of 43.6 GPa [40]. Refractive-index-matched infiltration of delignified wood produces highly anisotropic transparent and compressed-wood composites that combine load bearing with optical function [41,42]. The route extends naturally to low-value and fast-growing feedstocks, which chemical treatment and densification convert into high-performance structural materials, widening the usable resource base [22]. Mechanistic corroboration accumulates alongside these products. Pressure-mediated reconstruction of the hydrogen-bond network in moulded cellulose bulk materials has driven compressive strength as high as 575.3 MPa at ambient temperature, showing that densification acts in large part through interchain bonding [43]. *In-situ* synchrotron measurements of cellulose lattice strain further confirm that delignification and densification reshape stress transfer within the wall [44]. DES-assisted *in-situ* modification can also lock the densified geometry [45], a bridge to the dimensional-stability questions treated later, and reviews of delignified cellulose scaffolds place this whole material family within a common processing–mechanics framework [19,21]. The same logic underlies its adhesive-free and multifunctional variants. Partial dissolution of the fibre surface with an ionic liquid welds neighbouring cells directly, binding delignified wood into all-wood composites that need no external adhesive [32]. Pairing delignification with ionic-liquid treatment and densification yields laminates that carry hydrophobicity, flame retardancy or thermal function alongside their mechanical role [33]. Across this family the design principle is invariant: remove enough matrix to consolidate, retain or reintroduce enough binder to bond. Only the chemistry and the added function change.

Translational momentum now comes from two directions: recyclable green solvents that lower the environmental cost of delignification [31], and the demonstrated upgrading of abundant low-value species that broadens the feedstock base [22]. What remains unresolved is quantitative and cross-cutting. The optimal delignification degree is still calibrated species by species rather than predicted from wall composition. The threshold at which removal shifts from reorganizing to damaging the crystalline region is not generally defined [29]. The energy and cycle time of hot-pressing remain obstacles to scale that the softening-and-pressing paradigm has not itself resolved [35]. These three open questions, where to

CC BY

stop removing, how hard to press, and at what cost, motivate the pressure-free and reconstitution routes examined next, and the scale-by-scale mechanistic account that follows them.

3.2. Beyond hot-pressing: self-densification and reconstitution/assembly

Densification need not proceed through uniform external hot-pressing. A spectrum of routes now substitutes capillary self-densification, fibre reorganization, bottom-up reconstitution and spatially programmed gradients for the press (Figure 4). Each lowers the energy cost of strengthening while opening paths to three-dimensional shaping and industrial scale-up [13,14]. The routes are best ordered by how far they reorganize the native tissue, and, correspondingly, how little they depend on applied pressure. This ordering runs from the pressure-free collapse of an intact wall (Figure 5) [14], through moldable reshaping [13], to full disassembly and reassembly [18], and finally to deliberate spatial programming of density [16]. Read this way, they populate the fibre-bundle and bulk rungs of the strengthening framework and complement the wall-scale route of the previous section.

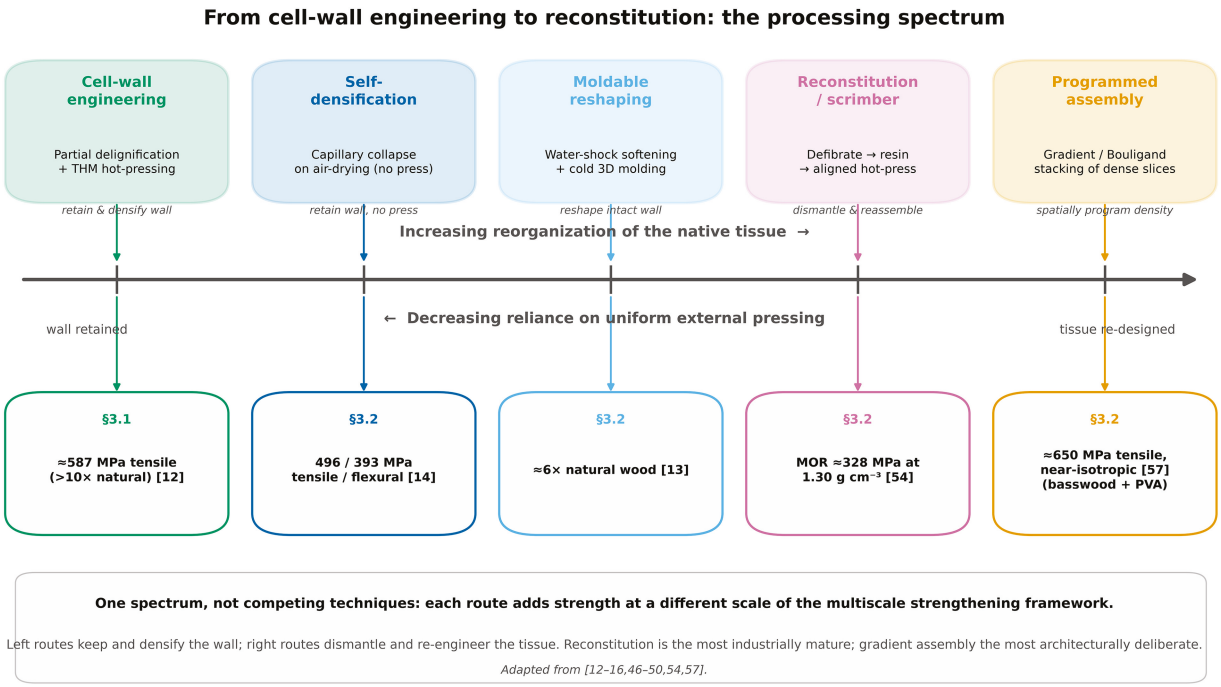


Figure 4. From cell-wall engineering to reconstitution: a processing spectrum ordered by how far each route reorganizes the native tissue and, in turn, how little it depends on uniform external pressing, with representative performance shown for each route. THM, thermo-hydro-mechanical; MOR, modulus of rupture; PVA, poly(vinyl alcohol)

At the least invasive end, self-densification consolidates wood without any press. Partial delignification followed by controlled swelling and air-drying lets capillary and surface-tension forces draw the softened walls together as water leaves. This pressure-free route yields an isotropically densified bulk with tensile and flexural strengths of 496 and 393 MPa respectively [14]. Steer that same air-drying differently and a delignified sheet builds a coexisting crystalline–amorphous dual-phase nanostructure, giving a foldable, origami-capable wood paper that is at once strong and tough [15]. The same capacity for cell-wall reconfiguration can be turned toward porosity rather than density. Sequential oxidation–reduction converts solid wood into an anisotropic elastic foam that recovers 60% of its transverse strain [46], and top-down reconstruction of the wall into arch-shaped lamellae yields a highly elastic, fatigue-resistant and conductive wood sponge [47]. Self-densification thus spans a continuous range, from dense structural solids to tunable elastic cellular materials, all reached without hot-pressing.

The physical driver is capillary action, not applied load. As water evaporates from the swollen, delignified wall, curved liquid surfaces form in the nanoscale pores, and the associated Laplace pressure pulls the pore walls inward. This self-generated compaction acts uniformly from all directions and so tends toward isotropic densification, in contrast to the strongly anisotropic solids left by uniaxial hot-pressing [14]. Because that driving force is distributed through the pore network instead of being transmitted from platens, thinness is not required, which is one reason the route suits bulk sections. The final structure depends on how the drying is controlled. Steering the collapse toward a coexisting crystalline–amorphous dual-phase nanostructure yields a material that is both strong and tough [15]. Arresting the collapse partway, or reconfiguring the wall into arched lamellae, preserves porosity and gives an elastic, recoverable cellular solid instead of a dense one [46,47]. The same capillary mechanism, differently arrested, accounts for the full span from super-strong bulk wood to reversible wood foams.

Retaining the wall while reshaping its geometry defines a second family of routes. Partial delignification followed by a brief water shock buckles and wrinkles the cell walls, making the wood pliable enough to be cold-moulded into three-dimensional forms. Once dried, these forms recover a strength roughly six times that of the natural material [13]. Reversible interlocking of delignified wood exploits the same wet-state plasticity for shaping and in-mould densification, and grading the treatment through the thickness produces bioinspired mechanical gradients with elastic moduli tunable from 5 to 35 GPa [48]. These routes preserve the continuous fibre architecture rather than dismantling it, so they combine formability with the intrinsic reinforcement of an intact, densified wall.

Reconstitution takes the opposite approach: it dismantles the tissue into fibres or bundles and reassembles it into an engineered solid. Delignified poplar can be reconstructed into a water-resistant, fibre-reinforced biocomposite (Figure 4) [49], and delignified wood reassembled with alkali lignin rebuilds the cell wall while improving both wet stability and toughness [50]. The most industrially mature version of this logic is scrimber. Wood or bamboo is defibrated into loosely connected bundles, impregnated with resin and consolidated at high density. Fast-growing poplar processed this way reaches structural grade, with properties matching or exceeding common engineered wood and bamboo [18] (Table 1; the four strategy families are compared in Table 2), and in bamboo scrimber the mechanical performance is dominated by the attained density [17]. Several processing refinements sharpen this control. Bundle knitting improves mat uniformity and cross-sectional density [51]. Phenol-formaldehyde felts consolidated near 1.15 g cm^{-3} optimize the property balance [52]. Roller-press impregnation drives resin deep and evenly, raising both dimensional stability and strength [53]. Resin loading is itself an optimizable variable: high-density bamboo scrimber peaks at a modulus of rupture of 327.9 MPa near 15 wt% resin, above which excess adhesive lowers crystallinity [54]. Refining the bundles by selectively removing hemicellulose before assembly improves strength, stiffness and water resistance further, fusing cell-wall engineering with reconstitution [55].

Spatial programming of density is the fourth and most architecturally deliberate route. Surface and asymmetric densification create a through-thickness density profile whose shape is governed by temperature, moisture and compression ratio [56]. Exploiting such asymmetry, single-sided gradient densification combined with an intracellular supramolecular network raises surface hardness 2.4-fold and flexural strength by 52% [16]. Programmable stacking of delignified wood veneers carries the idea further: 200 μm basswood veneers, delignified, infiltrated with poly(vinyl alcohol) (PVA) and densified layer by layer into a gradient Bouligand architecture, yield a macroscopically near-isotropic composite with a tensile strength of up to about 650 MPa at a density of 1.34 g cm^{-3} [57]. Because this material is a polymer-reinforced, wood-derived composite rather than densified solid wood, and basswood is not a typical plantation species, it marks the architectural upper bound of the route and is plotted with a separate symbol in the strength–density comparison of Section 5.2. Here strength comes not from raising density uniformly, but from placing dense, aligned or helically stacked material where the load demands it, which surpasses the ceiling of homogeneous densification.

The shape of the density profile is itself a controllable design variable. Under surface densification, the depth and steepness of the through-thickness density peak follow from the interplay of platen temperature, moisture content and compression ratio, which together set how far the softening front penetrates before the surface layer locks [56]. A single pressing then yields a hard, wear-resistant skin over a light, compliant core. Stacking thin delignified veneers before densification takes the control further still, replacing a monotonic profile with an arbitrary stacking sequence. Rotate successive layers through a small, constant angular increment and the helical Bouligand motif of biological armour reappears, spreading load across orientations so that the macroscopic response turns near-isotropic even though each layer stays anisotropic [57]. Gradient and laminate architectures thus add a spatial degree of freedom that uniform densification lacks: the same total mass of dense phase can be arranged to resist bending, impact or wear preferentially, which decouples the property distribution from the average density.

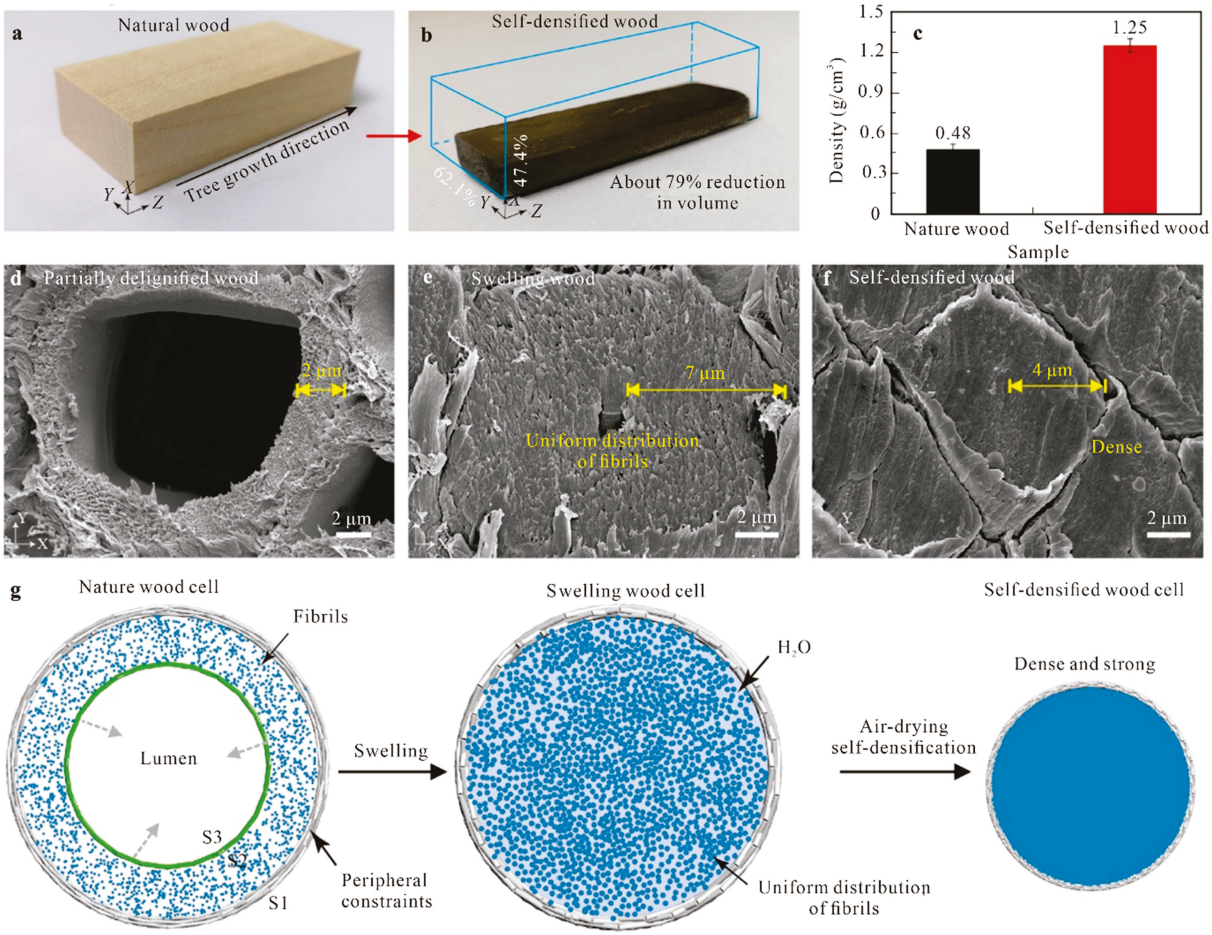


Figure 5. (Continued)

CC BY

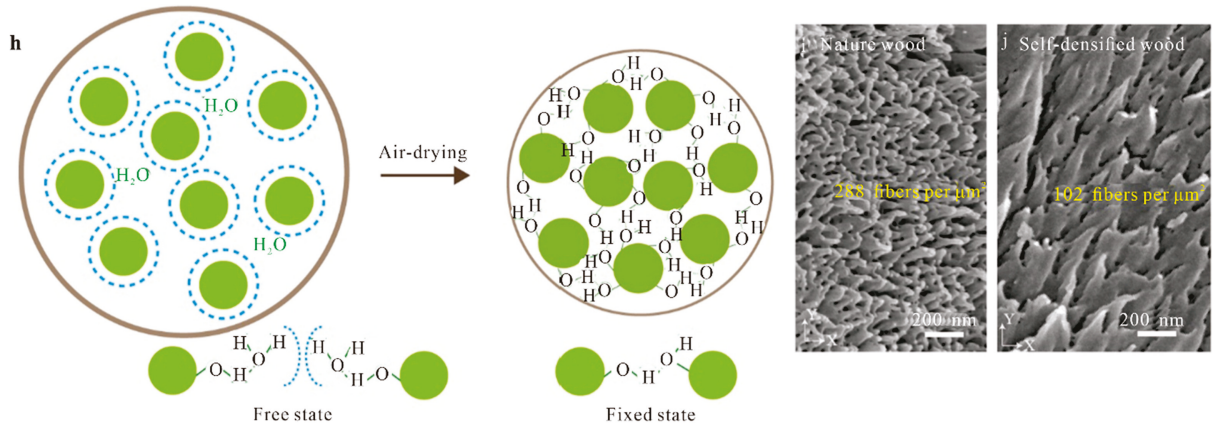


Figure 5. Microstructure and mechanism underlying the wood self-densification process. Photographs of (**a**) natural wood and (**b**) self-densified wood, indicating significant volume shrinkage. (**c**) Densities of the natural and self-densified wood. SEM images of (**d**) partially delignified wood cell, (**e**) swelling wood cell, and (**f**) self-densified wood cell. The cellulose fibrils first moved inward and filled the cell lumen, then self-densified into a dense and solid material. (**g**) Schematic illustration of self-densification process (S1, S2 and S3 are the outer layer, middle layer, and inner layer of the secondary wall of wood cell walls, respectively.). (**h**) Schematic illustration showing hydrogen bonding formation between adjacent cellulose fibrils during air-drying. The SEM images of (**i**) partially delignified wood cell wall featuring fibrils density of 288 fibers per μm^2, and (**j**) intermediate swelling wood cell wall featuring fibrils density of 102 fibers per μm^2. Adapted from Ref. [14]

Table 1: Mechanical performance of fast-growing wood species under different strengthening routes. Values are as reported in the cited primary sources; n.r. = not reported in the accessible source (no value is estimated). Density and tensile 496.1/flexural 392.7 for ref. [14] were extracted from the full-text portable document format (PDF) file; refs. [12,13] values are from published summaries of the primary papers; ref. [58] flexural strength was verified by the authors against the original article. sp. = specific strength; MOR = modulus of rupture; Nat. = Natural (untreated) wood; PF = phenol-formaldehyde resin; LiCl/DMAc = lithium chloride/N,N-dimethylacetamide. Microcrystalline-cellulose bulk material [22] is excluded (not a wood feedstock)

Species	Processing route	Density ($g\ cm^{-3}$)	Tensile (MPa)	Flexural/ MOR (MPa)	Modulus (GPa)	Set-recovery (%)	Ref.
Various wood	Partial delignification + hot-press	1.30 (nat. 0.43)	587	n.r.	n.r.	n.r.	[12]
Hardwood	Water-shock 3D molding	~0.75	~290 (sp. 386.8 MPa/($g\ cm^{-3}$))	n.r.	n.r.	n.r.	[13]
Wood	LiCl/DMAc swelling self-densification	1.25	496.1	392.7	n.r.	n.r.	[14]
Bamboo	High-density scrimber (15% PF)	1.30	n.r.	327.9 (MOR)	n.r.	n.r.	[54]
Poplar	Sodium-silicate impregnation + densification	n.r.	n.r.	322.5	n.r.	n.r.	[58]
Wood	DES *in-situ* modification + warm-press	n.r.	n.r.	173.7	9.1	4.7 (from 69.8)	[45]
Wood	Ultrathin film (partial delig. + hot-press)	n.r.	342	n.r.	43.65	n.r.	[40]
Poplar	Structure-retaining delig. + reconstitution	n.r.	n.r.	n.r.	n.r.	n.r.	[49]
Poplar	Scrimber (structural grade)	n.r.	n.r.	n.r.	n.r.	n.r.	[18]
Bamboo	Refined-bundle scrimber	n.r.	n.r.	n.r.	n.r.	n.r.	[55]

CC BY

Table 2. Comparison of the principal strengthening strategies for fast-growing wood: Representative processing conditions, density change, mechanical improvement, advantages and limitations. Representative values are drawn from the primary sources cited in Table 1 and in the text; See those references for full experimental conditions. THM = thermo-hydro-mechanical; DES = deep eutectic solvent; NaOH = sodium hydroxide; LiCl/DMAc = lithium chloride/N,N-dimethylacetamide

Strategy	Representative processing conditions	Density change (g cm^{-3})	Mechanical improvement	Advantages	Limitations	Ref.
Partial delignification + THM hot-pressing	Partial removal of lignin/ hemicellulose (alkaline sulfite, NaOH or DES), then hot-pressing above the lignin glass transition	0.43 -> 1.2–1.4 (about threefold)	Tensile up to ~587 MPa (>10× natural wood); ultrathin films 342 MPa/43.6 GPa	Very high strength; residual lignin self-bonds without added adhesive; broad species applicability	Batch pressing; thickness limited by through-thickness heat transfer; set-recovery on re-wetting	[12,40]
Pressure-free self-densification	Swelling of delignified wood (LiCl/DMAc or water-shock), then air-drying so fibrils close the lumen	up to ~1.25 (isotropic bulk)	Tensile ~290–496 MPa; specific strength ~387 MPa/(g cm^{-3})	No external pressing; near-isotropic; three-dimensionally moldable	Solvent handling; slow drying; scale-up not yet demonstrated	[13,14]
Reconstitution/ scrimber assembly	Defibration into fibre bundles or veneer, resin impregnation (e.g., 15% phenol-formaldehyde), re-assembly and hot-pressing	~1.30	MOR up to ~327.9 MPa (bamboo scrimber)	Already at industrial volume; uses low-value fast-growing feedstock; large components	Added resin raises cost and embodied emissions; interfaces moisture-sensitive	[18,49,50,54]
Spatially programmed/gradient densification	Localized swelling or impregnation (e.g., sodium silicate, DES) to set density or property gradients	graded (e.g., surface-densified M-profile)	MOR ~322.5 MPa (poplar); tailored stiffness; set-recovery cut to ~4.7%	Multifunctionality (fire, dimensional stability); tunable property distribution	Complex process control; long-term outdoor data scarce	[16,45,58,59]

Translational readiness varies sharply across this spectrum. Scrimber is already produced industrially from bamboo and fast-growing poplar, whereas self-densification and gradient assembly remain at laboratory to pilot scale. All three share a clear energy advantage over sustained hot-pressing, yet each carries its own unresolved problem. Reconstitution still leans on synthetic resin for interfacial bonding, which qualifies its sustainability claim. Pressure-free self-densification has yet to demonstrate scalable thickness and controllable isotropy. Gradient architectures lack predictive rules linking a programmed density profile to a target property distribution. Bonding without fossil resin, densifying uniformly without a press, designing a gradient by intent rather than trial: these questions set the agenda for the mechanistic analysis that follows and for the trade-off and durability considered thereafter.

4. Multiscale strengthening mechanisms

The strength that cell-wall engineering and reconstitution deliver is not the product of any single structural change. It is the coordinated output of four coupled length scales: molecular hydrogen bonding and crystallinity, cell-wall collapse and densification, fibre orientation, and interfacial load sharing.

4.1. Molecular scale: hydrogen bonding and crystallinity

At the finest scale, strengthening originates in the hydrogen-bond network and the crystalline order of cellulose. Densification roughly doubles the population of O(6)H $\cdots$ O(3′) intermolecular hydrogen bonds, and this increase correlates almost linearly with tensile strength (r = 0.952), which identifies interchain bonding as the primary molecular carrier of load [23] (Figure 6). Molecular-dynamics studies pinpoint the responsible donors: the hydroxyl groups at the C2 and C6 positions of the glucose units (OH2 and OH6) dominate the intermolecular bonding that governs the tensile strength of hydrated amorphous cellulose [60]. Backbone and hydrogen bonds act together, with the latter serving as a reversible lever that redistributes stress as the chain is stretched [61]. Thermo-hydro-mechanical treatment gains most of its strength by forming additional chain-internal and water-mediated hydrogen bonds [62]; how many form, and hence the chain stability and mechanical parameters they confer, tracks the local moisture and oxygen environment [63].

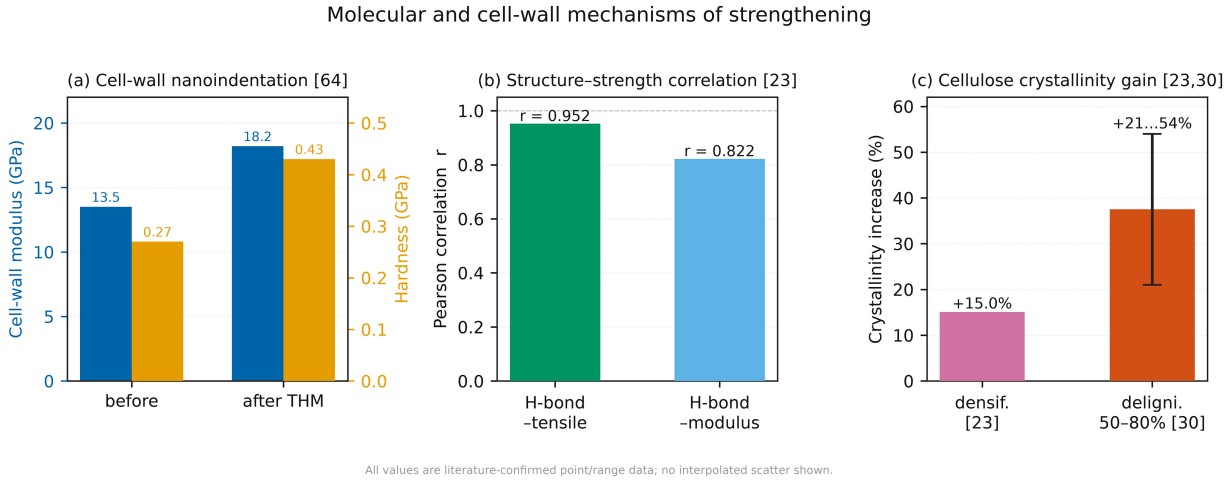


Figure 6. Molecular and cell-wall mechanisms of strengthening. (**a**) Longitudinal cell-wall modulus (left axis) and hardness (right axis) of earlywood measured by nanoindentation before and after thermo-hydro-mechanical (THM) densification of veneer [64]. (**b**) Pearson correlation coefficients between the increase in intermolecular hydrogen bonds and the tensile strength (r = 0.952) and modulus (r = 0.822) of densified wood [23]. (**c**) Increase in cellulose crystallinity after densification (+15.0%) [23] and after removal of 50–80% of the lignin (+21–54%; bar = midpoint, whisker = reported range) [29]. H-bond, hydrogen bond; Densif., densification; Deligni., delignification

These gains combine two distinct molecular changes, and separating them is worthwhile. The first is a change in hydrogen-bond population. Densification brings cellulose chains close enough for new interchain bonds to form, and what tracks the measured strength is the count of these intermolecular bonds, more than the intrachain ones [23,60]. The second is a change in crystalline order. As matrix polymers are removed and chains reorganize, the crystalline fraction rises, which stiffens the fibril. This is not the whole story, because the amorphous and interfacial hydrogen bonds carry a disproportionate share of the load transfer [61]. The two are coupled, since closer packing both adds bonds and improves registry, yet they respond differently to processing. A treatment can raise crystallinity without a matching strength gain if it fails to add the load-bearing intermolecular bonds.

4.2. Cell-wall scale: collapse and densification

X-ray diffraction of delignified, densified wood shows crystallinity rising and crystallite size decreasing while the crystalline orientation is preserved, as the interfibril spacing shortens and hydrogen bonding multiplies [65]. This is the wall-scale counterpart of the molecular picture above. Deep-eutectic-solvent pretreatment achieves the same consolidation without degrading crystallinity, so the strengthening draws on both cellulose hydrogen bonding and a lignin-induced fibre–lignin interface [66]. When porosity is removed entirely, as in two-step hot isostatic pressing that yields a non-porous, fully densified wood, void closure and wall stacking act in concert to raise strength [67]. The chemistry that enables collapse can be as minimal as a sodium-hydroxide-only pretreatment, which deacetylates hemicellulose and promotes chain migration, enhancing both plasticization and the subsequent hydrogen bonding across several species [28]. Nanoindentation, which resolves wall stiffness and hardness continuously with depth [68], records a rise in the longitudinal modulus of earlywood walls from 13.5 to 18.2 GPa and in hardness from 0.27 to 0.43 GPa after thermo-hydro-mechanical densification of veneer [64], so densification changes the wall itself and not only its void fraction. Cell-wall densification thus converts the molecular lever into a consolidated, low-porosity solid. It does so through routes whose chemistry differs but whose structural endpoint, a denser and more strongly bonded wall, is shared.

4.3. Fibre-bundle scale: orientation and microfibril angle

At the fibre-bundle scale, the orientation of cellulose microfibrils governs how efficiently the molecular and wall-scale strength is expressed along the loading axis. *In-situ* wide-angle X-ray scattering of *Pinus massoniana* shows the d004 spacing increasing and the microfibril angle decreasing under load, with the lattice strain varying linearly with macroscopic stress. This is direct evidence that the fibrils bear and transmit the applied load [69]. In low-MFA, high-stiffness spruce the same coupling appears as chain elongation and a reduction in the spacing between hydrogen-bonded sheets during tension [70]. Deformation is not purely elastic. Micropillar compression of the secondary cell wall of spruce latewood shows uneven out-of-plane bulging as the microfibrils buckle, followed by failure through a shear or kink band [71]. Cell walls recover after irreversible straining through a molecular stick-slip mechanism in the matrix, likened to nanoscale Velcro, which points to reversible sliding between fibrils that underlies the recoverability exploited by moldable and self-densifying routes [72]. Synchrotron micro-computed tomography that tracks individual cells quantifies how each contributes to the macroscopic deformation, bridging the single-cell and bulk responses [73].

The dynamic picture that emerges is one of progressive reorientation rather than rigid extension. Under axial load the microfibrils rotate toward the fibre axis, so the effective microfibril angle decreases as strain accumulates, and the measured lattice strain climbs in proportion to the applied stress. This signals that the crystalline cellulose takes up a larger share of the load as the wall stiffens [69]. The reorientation is partly reversible. The matrix that couples adjacent fibrils behaves like a molecular Velcro, letting fibrils slip and then re-register on unloading, which is why walls can recover much of an apparently irreversible deformation [72].

4.4. Interfacial and bulk scale: bonding and stress transfer

Atomic-force spectroscopy shows that an optimal residual lignin content of about 1.99% forms the most effective bonding layer, at which the strength peaks near 347.5 MPa. Too little lignin under-bonds the network, too much embrittles it [24]; this is the mechanistic counterpart of the removal-vs.-retention trade-off introduced as a processing choice in Section 3.1. Small-angle neutron scattering shows that stress transfer between microfibrils occurs chiefly as shear across their hydrogen-bonded contact interfaces, accompanied by viscous, water-facilitated stress relaxation [70]. The wood hemicelluloses make distinct biomechanical contributions to this fibrillar network, tuning its stiffness and extensibility and thereby regulating how those interfaces relax under load [25]. The interfacial network is moisture-sensitive: water molecules intrude into the hydrogen-bonded interfaces of microfibril bundles and swell

them, weakening the very contacts that carry the shear [74]. That the mechanism is general, and not specific to wood, is confirmed by hydrogen-bond-aided cellulose-scaffold/aramid composites, in which engineered hydrogen bonding builds a load-bearing interface between dissimilar fibres [75]. The interface is therefore the scale at which the strength assembled below is either transmitted to the bulk or dissipated.

5. Challenges and prospects

5.1. Cross-scale characterization and modelling

Viewed across all four scales, the levers act as a coupled system in which each amplifies the others. A single densification step at once shortens interchain distances and multiplies hydrogen bonds [23], collapses the porous wall [65,67], brings microfibrils into closer axial registry [69], and consolidates the load-bearing interface [24]. Attributing a macroscopic gain to any one mechanism in isolation therefore misrepresents its origin. This coupling explains why single-parameter correlations, however strong within one dataset, transfer poorly between species or processing routes, and why the predictive multiscale models needed to design, rather than discover, a target property remain the central unmet challenge [26]. It should be stressed that this coupling is at present inferred from convergent single-scale correlations rather than demonstrated by factorial experiments that isolate each lever, so supplying such decoupling evidence is itself part of that predictive-modelling gap. It also exposes a durability caveat. Because much of the molecular and interfacial gain is carried by hydrogen bonding, it is intrinsically vulnerable to moisture [74], a vulnerability whose engineering consequences the following section addresses. A concrete starting point is cellular-solid mechanics, which ties porous architecture to bulk response. In balsa, axial modulus and strength rise linearly with density, whereas in radial compression they vary nonlinearly, and models built on the cell structure and its deformation and failure mechanisms relate the two [76]. Densification moves wood along the same density axis, which makes this relation a natural baseline for interpreting densified wood, and structure–property relationships of balsa have likewise been mapped across a density gradient [77]. A review of wood mechanics from the nano- to the macro-scale reports size effects over about six orders of magnitude that follow a Hall-Petch-type relation, which shows that a single hierarchical description can span the scales [78]. Multiscale studies on other porous materials show how such a link can be made explicit. Numerical homogenization of triply periodic minimal surface (TPMS) metamaterials, for example, relates unit-cell configuration, constituent composition and volume fraction to effective coefficients at the microscale, and then carries these into a finite-element plate model that predicts the response at the macroscale [79]. That material is a piezoelectric lattice, so its numbers do not transfer to wood. The workflow does: resolve the pore architecture, homogenize it, then predict the component-scale behaviour. It offers a methodological template for predicting what a given degree of lumen collapse or density gradient will deliver. Quantifying the transfer functions that link one scale to the next, and stabilizing the bonds that carry the load, are the two problems on which a mechanistic, rather than empirical, strengthening of fast-growing wood now depends.

5.2. Lightweight–strength trade-off, durability and multifunctionality

The central cost is the lightweight–strength trade-off. Unless a resin or inorganic phase is introduced, densification adds no material: it raises density by removing void volume. Part of the strength gain therefore reflects the higher density itself. Gains harvested at the cell-wall and bulk scales are paid for in specific terms, and the most striking absolute strengths reported for densified and hot-pressed wood are reached at densities several times that of the native material [12] (Figure 7).

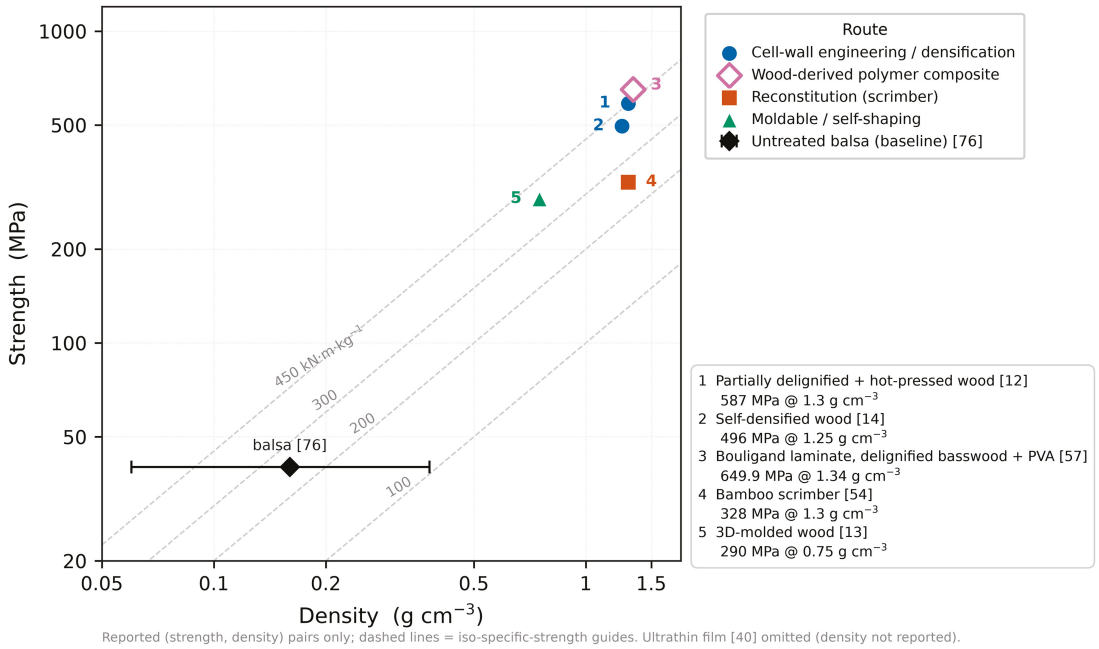


Figure 7. Strength–density design space of upgraded wood, with untreated balsa as the low-density baseline [76]. Filled symbols denote wood-feedstock routes: Partially delignified and hot-pressed wood [12] and self-densified wood [14] (circles), bamboo scrimber [54] (square) and 3D-molded wood [13] (triangle). The open diamond denotes a wood-derived polymer composite, a gradient Bouligand laminate of delignified basswood veneers infiltrated with poly(vinyl alcohol) (PVA) [57], and is shown separately from the wood-feedstock results. Dashed lines are iso-specific-strength guides; Only strength–density pairs reported in the cited sources are plotted

The instability that most limits application is set-recovery: compressed wood tends to spring back and swell when it takes up moisture, because the hydrogen bonds that lock the collapsed wall are themselves moisture-sensitive. Remedies therefore aim to fix the densified geometry against water. Impregnation with melamine–formaldehyde resin markedly reduces the set-recovery of densified poplar by cross-linking the collapsed structure (Figure 8) [80], and a thermotropic shape-memory polymer built *in situ* locks the compressed deformation while improving dimensional stability [81]. The pursuit of water resistance is closely related. Sodium-silicate impregnation of delignified poplar delivers a flexural strength of 322.5 MPa together with waterproofing and dimensional stability [58], while *in-situ* silica combined with aligned cellulose nanofibres yields a superhydrophobic structural wood with a contact angle of 159.4° and a strength of 384.2 MPa [82]. *In-situ* shape-fixation during deep-eutectic-solvent densification points in the same direction [45]. Across these strategies, stabilizing the load-bearing bonds against moisture is inseparable from preserving the strength they carry (Table 3).

The same impregnation and gradient platforms that stabilize the material can also make it multifunctional, turning durability treatment into added value. Fire safety is the most developed example. Impregnation with ammonium dihydrogen phosphate followed by densification forms a P–O–C char layer that raises the post-fire tensile and flexural strength by factors of 22.6 and 17.8 [83]. Remarkably, partial delignification and densification alone can generate a dense, self-formed char that increases post-fire compressive strength more than eightyfold without any added retardant [84]. Multifunctional laminates extend the idea. A mildly delignified, fluorinated-sulfonate-treated and densified wood combines a strength of 175.6 MPa with high toughness and flame retardancy [85], and densified laminates integrate hydrophobicity, flame retardancy and thermal insulation in a single material [86]. Gradient densification is the natural vehicle for such integration, concentrating protective or functional

CC BY

phases where they are most effective [16] (Table 3). Spatially selective delignification with epoxy infiltration, for its part, yields load-bearing transparent wood that transmits about 80% of light at a thermal conductivity of 0.24 W m^{-1} K^{-1} [87].

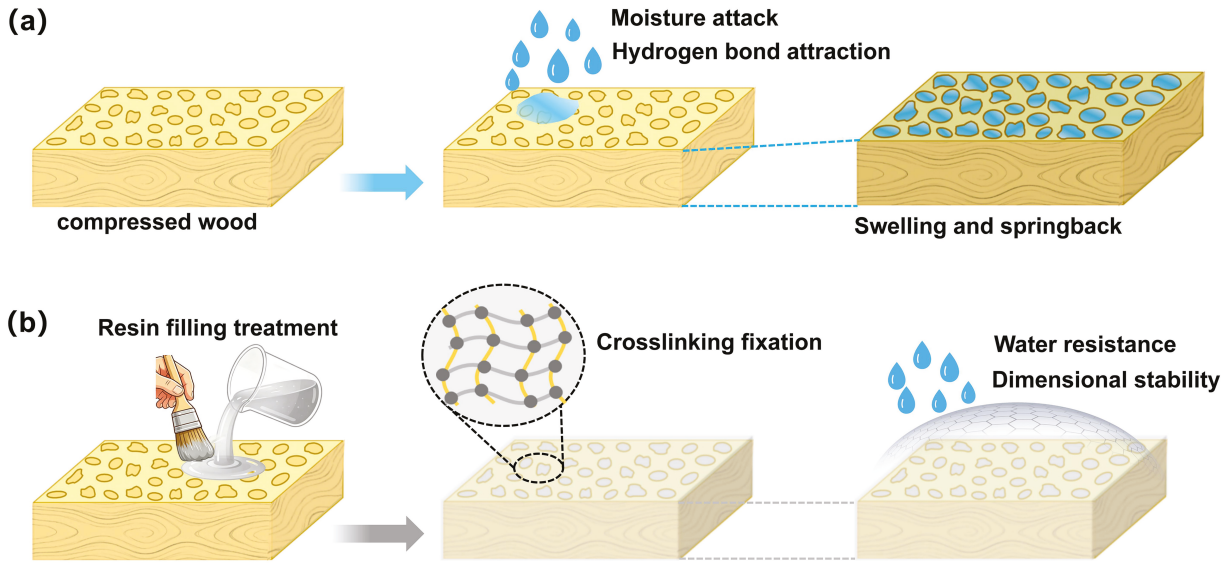


Figure 8. Set-recovery of densified wood and its suppression by resin impregnation (schematic). (**a**) When compressed wood is exposed to moisture, water breaks the hydrogen bonds that lock the collapsed cell walls, and the wood swells and springs back. (**b**) After resin filling treatment, the resin cures and cross-links within the densified structure, fixing the compressed geometry and giving water resistance and dimensional stability [80]

5.3. Applications, scale-up and sustainability of upgraded fast-growing wood

Moving strengthened fast-growing wood from a laboratory coupon to a structural component turns on three conditions that trail the strengthening science itself: manufacturing that scales, standards to evaluate the product against, and a sustainability case that survives full accounting. Mechanics is no longer the bottleneck; these three are. Whether the strength shown on small specimens becomes usable in construction depends on progress across all three, and reconstituted scrimber has already carried fast-growing wood to structural grade in industrial volume [18].

Manufacturing is the first of these conditions, and it remains the least mature. Most laboratory routes rely on static, batch hot-pressing, in which platens must be heated and often cooled for each load, so throughput is low and unit cost high. Heat transfer through the thickness is the binding constraint. In specimens more than a few millimetres thick the surface degrades before the core reaches the temperature needed to soften lignin; continuous industrial trials on poplar therefore densify only a sub-surface zone, leaving a characteristic M-shaped density profile rather than a uniformly densified board [59]. Uneven drying, limits on achievable thickness, and the cost of moulds and tooling for three-dimensional or gradient parts compound the problem, and natural defects such as knots further disturb the densification front. Treatment uniformity is a related obstacle on the chemical side: a capillary-driven self-flowing process delignifies wood six and four times more effectively than immersion and vacuum-pressure treatment, respectively, and does so more uniformly [88]. Continuous and belt-press systems adapted from panel manufacturing are the leading way past these limits, but transverse-compression products have stayed niche for over a century; reconstituted scrimber is so far the main exception to have reached genuine structural volume [18].

CC BY

Table 3. Strategies for dimensional stability, durability and integrated multifunctionality of densified fast-growing wood. Values are given as reported in the cited primary sources; n.r. = not reported in the accessible source (no value is estimated). Post-fire multipliers refer to the burnt untreated or unretarded reference of the cited study. Rows fall into four groups, dimensional stability, water resistance, fire resistance and multifunctional integration, of which the last two consolidate the quantitative content of the former gradient/multifunctionality figure. SiO_2 = silicon dioxide

Strategy	Mechanism	Functional/Durability effect	Accompanying mechanics	Ref.
DES *in-situ* modification + warm-press crosslinking	Crosslinks the collapsed wall to fix geometry	Set-recovery 69.8% -> 4.7%	Flexural 173.7 MPa	[45]
Melamine-formaldehyde impregnation	Resin cures within the densified structure	Set-recovery markedly reduced (value n.r.)	n.r.	[80]
***In-situ* thermo-responsive shape-memory polymer**	Locks compressed deformation on cooling	Compression locked; dimensional stability improved (n.r.)	n.r.	[81]
Roller-press phenol-formaldehyde impregnation	Deep, even resin penetration	Thickness/width swelling down 63%/35%	Strength & stability improved	[53]
Lignin back-fill scaffold stabilization	Re-deposited lignin stabilizes the scaffold	Water-resistant (value n.r.)	n.r.	[49,50]
Sodium-silicate impregnation	Inorganic phase fills and waterproofs the wall	Waterproof + dimensionally stable	Flexural 322.5 MPa	[58]
***In-situ* SiO2 + aligned cellulose nanofibres**	Superhydrophobic surface repels water	Contact angle 159.4 deg (dynamic 3 deg)	Strength 384.2 MPa	[82]
Ammonium-dihydrogen-phosphate + densification	*In-situ* P-O-C char layer	Post-fire tensile/flexural strength up to 22.6×/17.8×	Char-reinforced	[83]
Partial delignification + densification (no retardant)	Dense self-formed char on burning	Post-fire compressive strength >80×	No added flame retardant	[84]
Single-sided gradient densification + supramolecular network	Dense skin over lighter core	Surface hardness 2.4×; a spatial lever for function placement	Flexural strength +52%	[16]
Mild delignification + fluorinated sulfonate + densification	Multifunctional laminate	Flame-retardant + high toughness	Strength 175.6 MPa	[85]
Densified multifunctional laminate	Combines protective phases in one solid	Hydrophobic + flame-retardant + thermally insulating	Structural	[86]
Spatially selective delignification + epoxy infiltration	Transparent load-bearing wood	~80% optical transmittance; 0.24 W m^{-1} K^{-1}	Load-bearing	[87]

Durability in service is the second gap, and it is sharpest outdoors. Densification itself lowers water uptake and improves decay resistance by closing the porosity that moisture and fungi exploit, but the compressed geometry is metastable: on re-wetting it tends to spring back through set-recovery, so a densified part used outdoors must also be dimensionally locked against moisture. Chemical modification supplies that durability. Acetylation and furfurylation, both already at industrial scale, lower the equilibrium moisture content and confer resistance to fungi and weathering. Furfuryl-alcohol impregnation additionally plasticizes the wall during pressing and locks in the compressive set, so that modification and densification reinforce one another rather than competing [89]. Combined hydrophobic, flame-retardant and anti-fungal impregnation treatments extend the same logic toward

multifunctional exterior performance [86]. Weathering resistance under real ultraviolet and wetting-drying cycles, however, is still reported far less often than the initial mechanical gains, and long-term outdoor data on strengthened fast-growing wood remain scarce.

At the scale of buildings, that displacement benefit is substantial and increasingly well quantified. Substituting wood for steel and concrete in load-bearing elements can reduce whole-building emissions by roughly two-thirds relative to conventional construction [1], and life-cycle assessments of mass-timber construction find that reinforced-concrete buildings carry on the order of 40% higher embodied greenhouse-gas emissions than mass-timber alternatives [90]. Dynamic analyses that track the timing of biogenic carbon flows refine, and in some cases temper, these static estimates [91]. Global scenarios project that scaling mass-timber products could yield net reductions of 25.6–39.0 $GtCO_2e$ by 2100, alongside expanded forest area [2], and land-use modelling of a transition to timber cities maps the associated carbon and land consequences [3]. Building this demand on abundant, fast-growing, low-value species rather than on slow-grown timber is what keeps the resource base consistent with the projected scale [22]. Across all three conditions, the decisive step is to close the distance between promising small-coupon laboratory results and validated, code-compliant performance in full-scale structural members under service moisture, load and time.

6. Conclusions and outlook

Fast-growing wood can be transformed into lightweight structural materials through coordinated control of composition, cell-wall architecture, fibre alignment, and interfacial bonding. Partial delignification and densification can increase the density of load-bearing cell-wall material and create opportunities for stronger intermolecular interactions, whereas reconstitution and assembly routes can improve structural continuity and stress transfer at larger length scales. The resulting properties depend on coupled mechanisms rather than on any single processing step. Future studies should report processing conditions and test variables in a more standardized manner, particularly species, density, moisture content, loading direction, and test method. Progress toward moisture-stable interfaces, scalable manufacturing, and predictive multiscale structure-property models will be required before these materials can be deployed reliably in structural applications. A rigorous comparison of environmental burdens and end-of-life pathways will also be necessary to substantiate sustainability claims.

Acknowledgement: Not applicable.

Funding Statement: This work is supported by the Guangdong Forestry Science and Technology Innovation Project under Grant No. 2025KJCX011.

Author Contributions: Literature search and analysis: Lamei Li and Yixin Li; writing—original draft preparation: Minting Lai and Guijun Xie; writing—review and editing: Qiaoguang Li and Wanju Li. All authors reviewed and approved the final version of the manuscript.

Availability of Data and Materials: No new experimental data were generated in this review. All values discussed in the text, Tables 1–3 and Figures 4, 6 and 7 were extracted from the published sources cited in the reference list, and the source of each value is cited where it appears. The data-extraction sheet compiled for this review is available from the corresponding author on reasonable request.

Ethics Approval: Ethical approval was not required for this study because it is not involved any human experiments.

Conflicts of Interest: Given his role as an Editorial Board Member of this journal, Qiaoguang Li had no involvement in the peer review of this article and had no access to information regarding its peer review. Full responsibility for the editorial process for this article was delegated to another journal editor. The authors declare no other conflicts of interest.

CC BY

References

1. Himes A, Busby G. Wood buildings as a climate solution. Dev Built Environ. 2020;4(3):100030. doi:10.1016/j.dibe.2020.100030.
2. Lan K, Favero A, Yao Y, Mendelsohn RO, Wang HS. Global land and carbon consequences of mass timber products. Nat Commun. 2025;16(1):4864. doi:10.1038/s41467-025-60245-y.
3. Mishra A, Humpenöder F, Churkina G, Reyer CPO, Beier F, Bodirsky BL, et al. Land use change and carbon emissions of a transformation to timber cities. Nat Commun. 2022;13(1):4889. doi:10.1038/s41467-022-32244-w.
4. Chen C, Kuang Y, Zhu S, Burgert I, Keplinger T, Gong A, et al. Structure–property–function relationships of natural and engineered wood. Nat Rev Mater. 2020;5(9):642–66. doi:10.1038/s41578-020-0195-z.
5. Terzopoulou P, Kamperidou V, Barboutis I. Utilization potential of tree-of-heaven species biomass—a review. Appl Sci. 2023;13(16):9185. doi:10.3390/app13169185.
6. Baltunis BS, Wu HX, Powell MB. Inheritance of density, microfibril angle, and modulus of elasticity in juvenile wood of *Pinus radiata* at two locations in Australia. Can J For Res. 2007;37(11):2164–74. doi:10.1139/x07-061.
7. Su M, He J, Jia R, Wang Y. Multi-layered structure of wood cell wall among hybrid poplars and its affect on mechanical properties. Int J Biol Macromol. 2025;304(Pt 1):140784. doi:10.1016/j.ijbiomac.2025.140784.
8. Wang X, Zhao W, Zhang Y, Shi J, Shan S, Cai L. Exploring wood micromechanical structure: impact of microfibril angle and crystallinity on cell wall strength. J Build Eng. 2024;90(1):109452. doi:10.1016/j.jobe.2024.109452.
9. Marini LJ, Cavalheiro RS, Almeida De Araujo V, Cortez-Barbosa J, de Campos CI, Molina JC, et al. Estimation of mechanical properties in *Eucalyptus* woods towards physical and anatomical parameters. Constr Build Mater. 2022;352(128):128824. doi:10.1016/j.conbuildmat.2022.128824.
10. Gibson LJ. The hierarchical structure and mechanics of plant materials. J R Soc Interface. 2012;9(76):2749–66. doi:10.1098/rsif.2012.0341.
11. Fratzl P, Weinkamer R. Nature's hierarchical materials. Prog Mater Sci. 2007;52(8):1263–334. doi:10.1016/j.pmatsci.2007.06.001.
12. Song J, Chen C, Zhu S, Zhu M, Dai J, Ray U, et al. Processing bulk natural wood into a high-performance structural material. Nature. 2018;554(7691):224–8. doi:10.1038/nature25476.
13. Xiao S, Chen C, Xia Q, Liu Y, Yao Y, Chen Q, et al. Lightweight, strong, moldable wood via cell wall engineering as a sustainable structural material. Science. 2021;374(6566):465–71. doi:10.1126/science.abg9556.
14. Huang D, Li J, Li S, Hu J, Cao Z, Guo Y, et al. Self-densified super-strong wood. J Bioresour Bioprod. 2025;10(2):199–208. doi:10.1016/j.jobab.2025.03.001.
15. Tang J, Wu L, Fan X, Dong X, Li X, Xie Y, et al. Superstrong, sustainable, origami wood paper enabled by dual-phase nanostructure regulation in cell walls. Sci Adv. 2024;10(30):eado5142. doi:10.1126/sciadv.ado5142.
16. Fan Q, Zhang X, Chen C, Hao X, Liu Z, Ou R, et al. Biomimetic versatile wood hybrids with gradient structure towards lightweight, high strength, fire-retardant, and deterioration-resistant materials. Compos Part B Eng. 2024;280(6442):111483. doi:10.1016/j.compositesb.2024.111483.
17. Kumar A, Vlach T, Laiblova L, Hrouda M, Kasal B, Tywoniak J, et al. Engineered bamboo scrimber: influence of density on the mechanical and water absorption properties. Constr Build Mater. 2016;127(2):815–27. doi:10.1016/j.conbuildmat.2016.10.069.
18. He MJ, Zhang J, Li Z, Li ML. Production and mechanical performance of scrimber composite manufactured from poplar wood for structural applications. J Wood Sci. 2016;62(5):429–40. doi:10.1007/s10086-016-1568-1.

19. Keplinger T, Wittel FK, Rüggeberg M, Burgert I. Wood derived cellulose scaffolds—processing and mechanics. Adv Mater. 2021;33(28):2001375. doi:10.1002/adma.202001375.
20. Cabral JP, Kafle B, Subhani M, Reiner J, Ashraf M. Densification of timber: a review on the process, material properties, and application. J Wood Sci. 2022;68(1):20. doi:10.1186/s10086-022-02028-3.
21. Kumar A, Jyske T, Petrič M. Delignified wood from understanding the hierarchically aligned cellulosic structures to creating novel functional materials: a review. Adv Sustain Syst. 2021;5(5):2000251. doi:10.1002/adsu.202000251.
22. Dong X, Gan W, Shang Y, Tang J, Wang Y, Cao Z, et al. Low-value wood for sustainable high-performance structural materials. Nat Sustain. 2022;5(7):628–35. doi:10.1038/s41893-022-00887-8.
23. Li K, Zhao L, Ren J, He B. Interpretation of strengthening mechanism of densified wood from supramolecular structures. Molecules. 2022;27(13):4167. doi:10.3390/molecules27134167.
24. Li K, Zhao L, Ren J, He B. Lignin's effect on cellulose fiber bonding and inter-fiber interface design for enhancing densified wood. Carbohydr Polym. 2025;359(11−12):123573. doi:10.1016/j.carbpol.2025.123573.
25. Berglund J, Mikkelsen D, Flanagan BM, Dhital S, Gaunitz S, Henriksson G, et al. Wood hemicelluloses exert distinct biomechanical contributions to cellulose fibrillar networks. Nat Commun. 2020;11(1):4692. doi:10.1038/s41467-020-18390-z.
26. Song R, Deng F, Liang X, Song J, Shen S, Li T. A multiscale mechanics model for elastic properties of densified wood. J Mech Phys Solids. 2024;191(5):105761. doi:10.1016/j.jmps.2024.105761.
27. Mania P, Kupfernagel C, Curling S. Densification of delignified wood: influence of chemical composition on wood density, compressive strength, and hardness of Eurasian aspen and Scots pine. Forests. 2024;15(6):892. doi:10.3390/f15060892.
28. Andze L, Nefjodovs V, Zoldners J, Milbreta U, Skute M, Vecbiskena L, et al. NaOH-only pretreated wood densification: a simplified sulfite-free route across wood species. Polymers. 2026;18(3):312. doi:10.3390/polym18030312.
29. Alqrinawi H, Ahmed B, Wu Q, Lin H, Kameshwar S, Shayan M. Effect of partial delignification and densification on chemical, morphological, and mechanical properties of wood: structural property evolution. Ind Crops Prod. 2024;213(18):118430. doi:10.1016/j.indcrop.2024.118430.
30. Mao Y, Tarhanli I, Owen G, Lee CS, Senses E, Binner E. Comparisons of alkali, organosolv and deep eutectic solvent pre-treatments on the physiochemical changes and lignin recovery of oak and pine wood. Ind Crops Prod. 2025;226:120614. doi:10.1016/j.indcrop.2025.120614.
31. Fan Z, Sun H, Zhang L, Zhao X, Hu Y. Lightweight, high-strength wood prepared by deep eutectic solvent treatment as a green structural material. ACS Sustain Chem Eng. 2022;10(29):9600–11. doi:10.1021/acssuschemeng.2c02606.
32. Khakalo A, Tanaka A, Korpela A, Hauru LKJ, Orelma H. All-wood composite material by partial fiber Surface Dissolution with an ionic liquid. ACS Sustain Chem Eng. 2019;7(3):3195–202. doi:10.1021/acssuschemeng.8b05059.
33. Khakalo A, Tanaka A, Korpela A, Orelma H. Delignification and ionic liquid treatment of wood toward multifunctional high-performance structural materials. ACS Appl Mater Interfaces. 2020;12(20):23532–42. doi:10.1021/acsami.0c02221.
34. Li Y, Fu Q, Yu S, Yan M, Berglund L. Optically transparent wood from a nanoporous cellulosic template: combining functional and structural performance. Biomacromolecules. 2016;17(4):1358–64. doi:10.1021/acs.biomac.6b00145.
35. Sandberg D, Haller P, Navi P. Thermo-hydro and thermo-hydro-mechanical wood processing: an opportunity for future environmentally friendly wood products. Wood Mater Sci Eng. 2013;8(1):64–88. doi:10.1080/17480272.2012.751935.

36. Navi P, Girardet F. Effects of thermo-hydro-mechanical treatment on the structure and properties of wood. Holzforschung. 2000;54(3):287–93. doi:10.1515/hf.2000.048.
37. Frey M, Widner D, Segmehl JS, Casdorff K, Keplinger T, Burgert I. Delignified and densified cellulose bulk materials with excellent tensile properties for sustainable engineering. ACS Appl Mater Interfaces. 2018;10(5):5030–7. doi:10.1021/acsami.7b18646.
38. Frey M, Schneider L, Masania K, Keplinger T, Burgert I. Delignified wood-polymer interpenetrating composites exceeding the rule of mixtures. ACS Appl Mater Interfaces. 2019;11(38):35305–11. doi:10.1021/acsami.9b11105.
39. Li Y, Fu Q, Rojas R, Yan M, Lawoko M, Berglund L. Lignin-retaining transparent wood. ChemSusChem. 2017;10(17):3445–51. doi:10.1002/cssc.201701089.
40. Gan W, Chen C, Kim HT, Lin Z, Dai J, Dong Z, et al. Single-digit-micrometer thickness wood speaker. Nat Commun. 2019;10(1):5084. doi:10.1038/s41467-019-13053-0.
41. Zhu M, Song J, Li T, Gong A, Wang Y, Dai J, et al. Highly anisotropic, highly transparent wood composites. Adv Mater. 2016;28(26):5181–7. doi:10.1002/adma.201600427.
42. Wang Y, Wu Y, Yang F, Yang L, Wang J, Zhou J, et al. A highly transparent compressed wood prepared by cell wall densification. Wood Sci Technol. 2022;56(2):669–86. doi:10.1007/s00226-022-01372-3.
43. Liang X, Guo Y, Yan J, Bian T, Wang C, Zhang H, et al. Pressure-mediated reconstruction of hydrogen bonding networks under ambient temperature towards high-strength cellulosic bulk materials. Cellulose. 2024;31(9):5461–77. doi:10.1007/s10570-024-05936-3.
44. Spies PA, Keplinger T, Horbelt N, Reppe F, Scoppola E, Eder M, et al. Cellulose lattice strains and stress transfer in native and delignified wood. Carbohydr Polym. 2022;296(3):119922. doi:10.1016/j.carbpol.2022.119922.
45. Ran Y, Lu D, Jiang J, Huang Y, Wang W, Cao J. Deep eutectic solvents-assisted wood densification: a promising strategy for shape-fixation. Chem Eng J. 2023;471(5):144476. doi:10.1016/j.cej.2023.144476.
46. Shi X, Bi R, Wan Z, Jiang F, Rojas OJ. Solid wood modification toward anisotropic elastic and insulative foam-like materials. ACS Nano. 2024;18(11):7959–71. doi:10.1021/acsnano.3c10650.
47. Dai XJ, Wang X, Hu JH, Jiang P, Wang XQ. Highly elastic and conductive lamellar wood sponge via cell wall reconfiguration toward smart multifunctional applications. Nanomicro Lett. 2026;18(1):171. doi:10.1007/s40820-025-02016-4.
48. Frey M, Biffi G, Adobes-Vidal M, Zirkelbach M, Wang Y, Tu K, et al. Tunable wood by reversible interlocking and bioinspired mechanical gradients. Adv Sci. 2019;6(10):1802190. doi:10.1002/advs.201802190.
49. Movahedi-Rad AV, Ritter M, Kindler RO, Burgert I, Panzarasa G. Reconstructing poplar wood into a high-performance fiber-reinforced biocomposite. ACS Sustain Chem Eng. 2024;12(40):14694–703. doi:10.1021/acssuschemeng.4c04652.
50. Gu F, Niu X, Zhang D, Cai Z, Wang W, Song J, et al. Plant cell wall reconstruction towards enhancing moisture stability and toughness by assembling delignified wood with alkali lignin. Wood Sci Technol. 2024;58(3):923–39. doi:10.1007/s00226-024-01552-3.
51. He S, Xu J, Wu ZX, Yu H, Chen YH, Song JG. Effect of bamboo bundle knitting on enhancing properties of bamboo scrimber. Eur J Wood Wood Prod. 2018;76(3):1071–8. doi:10.1007/s00107-017-1263-y.
52. Bao M, Li N, Huang C, Chen Y, Yu W, Yu Y. Fabrication, physical–mechanical properties and morphological characterizations of novel scrimber composite. Eur J Wood Wood Prod. 2019;77(5):741–7. doi:10.1007/s00107-019-01440-9.

53. Gao Q, Lin Q, Huang Y, Hu J, Yu W. High-performance wood scrimber prepared by a roller-pressing impregnation method. Constr Build Mater. 2023;368:130404. doi:10.1016/j.conbuildmat.2023.130404.
54. Yang Z, Meng X, Zeng G, Wei J, Wang C, Yu W. Effect of resin content on the structure, water resistance and mechanical properties of high-density bamboo scrimbers. Polymers. 2024;16(6):797. doi:10.3390/polym16060797.
55. Liu C, Wu X, Li X, Liu X. Structure and physical properties of high-density bamboo scrimber made from refined bamboo bundles. Eur J Wood Wood Prod. 2024;82(6):1867–78. doi:10.1007/s00107-024-02120-z.
56. Rautkari L, Laine K, Laflin N, Hughes M. Surface modification of Scots pine: the effect of process parameters on the through thickness density profile. J Mater Sci. 2011;46(14):4780–6. doi:10.1007/s10853-011-5388-9.
57. Wang Q, Wu B, Yu S, Xiong R. Superstrong and supertough biomimetic nanocellulose composites with gradient bouligand architecture. Nat Commun. 2026;17(1):5621. doi:10.1038/s41467-026-72343-6.
58. Kuai B, Wang Z, Gao J, Tong J, Zhan T, Zhang Y, et al. Development of densified wood with high strength and excellent dimensional stability by impregnating delignified poplar by sodium silicate. Constr Build Mater. 2022;344(18):128282. doi:10.1016/j.conbuildmat.2022.128282.
59. Sadatnezhad SH, Khazaeian A, Sandberg D, Tabarsa T. Continuous surface densification of wood: a new concept for large-scale industrial processing. BioResources. 2017;12(2):3122–32. doi:10.15376/biores.12.2.3122-3132.
60. Nakamura T, Ishiyama T. Molecular dynamics study of hydrogen bond structure and tensile strength for hydrated amorphous cellulose. Biomacromolecules. 2024;25(11):7249–59. doi:10.1021/acs.biomac.4c00950.
61. Altaner CM, Thomas LH, Fernandes AN, Jarvis MC. How cellulose stretches: synergism between covalent and hydrogen bonding. Biomacromolecules. 2014;15(3):791–8. doi:10.1021/bm401616n.
62. Ouyang F, Wang W. Effect of thermo-hydro-mechanical treatment on mechanical properties of wood cellulose: a molecular dynamics simulation. Forests. 2022;13(6):903. doi:10.3390/f13060903.
63. Guo Y, Wang W, Jiang X. Molecular dynamics study on mechanical properties of cellulose with water molecules diffusion behavior at different oxygen concentrations. Forests. 2023;14(2):371. doi:10.3390/f14020371.
64. Bustos Avila C, Gacitúa Escobar W, Cloutier A, Fang CH, Valenzuela Carrasco P. Densification of wood veneers combined with oil-heat treatment. part III: cell wall mechanical properties determined by nanoindentation. BioResources. 2012;7(2):1525–32. doi:10.15376/biores.7.2.1525-1532.
65. Huang W, Jin Y, Guo Y, Deng J, Yu H, He B. Fabrication of high-performance densified wood via high-pressure steam treatment and hot-pressing. Polymers. 2024;16(7):939. doi:10.3390/polym16070939.
66. Gondaliya AM, Hoque M, Raghunath S, Foster EJ. Green and sustainable fabrication of DES-pretreated high-strength densified wood. Wood Sci Technol. 2024;58(5–6):1901–23. doi:10.1007/s00226-024-01594-7.
67. Maturana JC, Guindos P, Lagos J, Arroyave C, Echeverría F, Correa E. Two-step hot isostatic pressing densification achieved non-porous fully-densified wood with enhanced physical and mechanical properties. Sci Rep. 2023;13(1):14324. doi:10.1038/s41598-023-41342-8.
68. Tze WTY, Wang S, Rials TG, Pharr GM, Kelley SS. Nanoindentation of wood cell walls: continuous stiffness and hardness measurements. Compos Part A Appl Sci Manuf. 2007;38(3):945–53. doi:10.1016/j.compositesa.2006.06.018.

69. Guo F, Wang J, Liu W, Hu J, Chen Y, Zhang X, et al. Role of microfibril angle in molecular deformation of cellulose fibrils in *Pinus massoniana* compression wood and opposite wood studied by *in-situ* WAXS. Carbohydr Polym. 2024;334(3):122024. doi:10.1016/j.carbpol.2024.122024.
70. Thomas LH, Altaner CM, Forsyth VT, Mossou E, Kennedy CJ, Martel A, et al. Nanostructural deformation of high-stiffness spruce wood under tension. Sci Rep. 2021;11(1):453. doi:10.1038/s41598-020-79676-2.
71. Adusumalli RB, Raghavan R, Ghisleni R, Zimmermann T, Michler J. Deformation and failure mechanism of secondary cell wall in Spruce late wood. Appl Phys A. 2010;100(2):447–52. doi:10.1007/s00339-010-5847-1.
72. Keckes J, Burgert I, Frühmann K, Müller M, Kölln K, Hamilton M, et al. Cell-wall recovery after irreversible deformation of wood. Nat Mater. 2003;2(12):810–4. doi:10.1038/nmat1019.
73. Sanabria SJ, Baensch F, Zauner M, Niemz P. *In-situ* quantification of microscopic contributions of individual cells to macroscopic wood deformation with synchrotron computed tomography. Sci Rep. 2020;10(1):21615. doi:10.1038/s41598-020-78028-4.
74. Paajanen A, Zitting A, Rautkari L, Ketoja JA, Penttilä PA. Nanoscale mechanism of moisture-induced swelling in wood microfibril bundles. Nano Lett. 2022;22(13):5143–50. doi:10.1021/acs.nanolett.2c00822.
75. Han X, Wu W, Wang J, Tian Z, Jiang S. Hydrogen-bonding-aided fabrication of wood derived cellulose scaffold/aramid nanofiber into high-performance bulk material. Materials. 2021;14(18):5444. doi:10.3390/ma14185444.
76. Borrega M, Gibson LJ. Mechanics of *Balsa* (*Ochroma pyramidale*) wood. Mech Mater. 2015;84:75–90. doi:10.1016/j.mechmat.2015.01.014.
77. Zhao W, Zeng Z, Cai Q, Rao J, Li M, Yan W, et al. Structure-property relationships of *Balsa* wood across a density gradient for vacuum insulation performance. Eur J Wood Wood Prod. 2025;84(1):9. doi:10.1007/s00107-025-02365-2.
78. Golovin YI, Gusev AA, Golovin DY, Matveev SM, Vasyukova IA. Multiscale mechanical performance of wood: from nano- to macro-scale across structure hierarchy and size effects. Nanomater. 2022;12(7):1139. doi:10.3390/nano12071139.
79. Zhang Y, Zhao S, Guo X, Zhang Y, Ni Z, Zhang Y, et al. Multiscale electro-mechanical behaviours of TPMS piezoelectric metamaterials. Compos Struct. 2026;386:120289. doi:10.1016/j.compstruct.2026.120289.
80. Lykidis C, Kotrotsiou K, Tsichlakis A. Reducing set-recovery of compressively densified poplar wood by impregnation–modification with melamine–formaldehyde resin. Wood Mater Sci Eng. 2020;15(5):269–77. doi:10.1080/17480272.2019.1594365.
81. Zhang W, Zhou J, Cao Z, Wu X, Wang H, Han S, et al. *In situ* construction of thermotropic shape memory polymer in wood for enhancing its dimensional stability. Polymers. 2022;14(4):738. doi:10.3390/polym14040738.
82. Li Y, Chen C, Song J, Yang C, Kuang Y, Vellore A, et al. Strong and superhydrophobic wood with aligned cellulose nanofibers as a waterproof structural material. Chin J Chem. 2020;38(8):823–9. doi:10.1002/cjoc.202000032.
83. Fan C, Gao Y, Li Y, Yan L, Zhu D, Guo S, et al. A flame-retardant densified wood as robust and fire-safe structural material. Wood Sci Technol. 2023;57(1):111–34. doi:10.1007/s00226-022-01415-9.
84. Gan W, Chen C, Wang Z, Song J, Kuang Y, He S, et al. Dense, self-formed char layer enables a fire-retardant wood structural material. Adv Funct Mater. 2019;29(14):1807444. doi:10.1002/adfm.201807444.

85. Han X, Wang X, Tian W, Wang Y, Wang J, Lam F, et al. A strong, tough and fire-retardant biomimetic multifunctional wooden laminate. Polymers. 2023;15(20):4063. doi:10.3390/polym15204063.
86. Tang G, Fu C, Zhen X, Guan M, Wang X, Deng D, et al. Multi-functional densified wood laminates with hydrophobicity, anti-flammability, and thermal insulation for structural applications. Ind Crops Prod. 2025;234(1):121520. doi:10.1016/j.indcrop.2025.121520.
87. Mi R, Chen C, Keplinger T, Pei Y, He S, Liu D, et al. Scalable aesthetic transparent wood for energy efficient buildings. Nat Commun. 2020;11(1):3836. doi:10.1038/s41467-020-17513-w.
88. Wang X, Shi SQ. Bioinspired self-flowing wood chemical treatment. Nat Commun. 2025;16(1):542. doi:10.1038/s41467-024-55782-x.
89. Sandberg D, Kutnar A, Mantanis G. Wood modification technologies—a review. IForest. 2017;10(6):895–908. doi:10.3832/ifor2380-010.
90. Duan Z, Huang Q, Zhang Q. Life cycle assessment of mass timber construction: a review. Build Environ. 2022;221:109320. doi:10.1016/j.buildenv.2022.109320.
91. Lan K, Kelley SS, Nepal P, Yao Y. Dynamic life cycle carbon and energy analysis for cross-laminated timber in the Southeastern United States. Environ Res Lett. 2020;15(12):124036. doi:10.1088/1748-9326/abc5e6.

Received: 04 August 2026; Accepted: 29 October 2026; Published: XX xxx 2026